LA-UR- 09-06497

Approved for public release; distribution is unlimited.

Title:	Mobilization of Colloidal Particles by Low-Frequency Dynamic Stress Stimulation
Author(s):	Richard E. Beckham, Amr I. Abdel-Fattah, Peter M. Roberts, Reem Ibrahim, and Sowmitri Tarimala
Intended for:	Langmuir

Los Alamos
NATIONAL LABORATORY
EST. 1943

Los Alamos National Laboratory, an affirmative action/equal opportunity employer, is operated by the Los Alamos National Security, LLC for the National Nuclear Security Administration of the U.S. Department of Energy under contract DE-AC52-06NA25396. By acceptance of this article, the publisher recognizes that the U.S. Government retains a nonexclusive, royalty-free license to publish or reproduce the published form of this contribution, or to allow others to do so, for U.S. Government purposes. Los Alamos National Laboratory requests that the publisher identify this article as work performed under the auspices of the U.S. Department of Energy. Los Alamos National Laboratory strongly supports academic freedom and a researcher's right to publish; as an institution, however, the Laboratory does not endorse the viewpoint of a publication or guarantee its technical correctness.

Form 836 (7/06)

Mobilization of Colloidal Particles by Low-Frequency Dynamic Stress Stimulation

Richard E. Beckham, Amr I. Abdel-Fattah, Peter M. Roberts, Reem Ibrahim, and Sowmitri Tarimala*

Los Alamos National Laboratory, Los Alamos, NM 87545, USA

rbeckham@lanl.gov, amr2450@lanl.gov, proberts@lanl.gov, reem@lanl.gov, and tarimala@lanl.gov

Abstract

Naturally occurring seismic events and artificially generated low-frequency (1 to 500 Hertz) elastic waves have been observed to alter the production rates of oil and water wells, sometimes increasing and sometimes decreasing production, and to influence the turbidity of surface and well water. The decreases in production are of particular concern – especially when artificially generated elastic waves are applied as a method for enhanced oil recovery. The exact conditions that result in a decrease in production remain unknown. While the underlying environment is certainly complex, the observed increase in water well turbidity after natural seismic events suggests the existence of a mechanism that can affect both the subsurface flow paths and mobilization of in-situ colloidal particles.

This paper explores the macroscopic and microscopic effects of low-frequency dynamic stress stimulations on the release of colloidal particles from an analog core representing an infinitesimal section along the propagation paths of an elastic wave. Experiments on a column packed with 1-mm

* To whom correspondence should be addressed. E-mail: amr2450@lanl.gov

borosilicate beads and loaded with polystyrene microspheres demonstrate that axial mechanical stress oscillations enhance the mobilization of captured microspheres. Increasing the amplitude of the oscillations increases the number of microspheres released and can also result in cyclical spikes in effluent microsphere concentration during stimulation. Under a prolonged period of stimulation, the cyclical effluent spikes coincided with fluctuations in the column pressure data, and continue at a diminished level after stimulation. This behavior can be attributed to rearrangements of the beads in the column, resulting in possible changes to the void space and/or tortuosity of the packing. Optical microscopy observations of the beads during low frequency oscillations reveal that individual beads rotate, thereby rubbing against each other and scraping away portions of the adsorbed microspheres. These results support the theory that mechanical interactions between porous matrix grains are important mechanisms in flow path alteration and the mobilization of naturally occurring colloidal particles during elastic wave stimulation. These results also point to both continuous and discrete, en masse releases of colloidal particles, perhaps due to circulation cells within the packing material.

Introduction

The effects of elastic waves – both naturally occurring and artificial – on the mobilization of colloidal particles and alteration of subsurface flow pathways are of concern for many applications including oil recovery, subsurface transport of contaminants, leakage of CO_2 geologic sequestration reservoirs, and remediation of contaminated aquifers. Natural seismic events and artificially induced elastic wave stimulations have been observed to alter oil well[1, 2] and water well[3] production. In particular, artificially applied low-frequency elastic waves [$\leq$ 500 Hertz (Hz)] have been studied extensively as a method for improving oil well production.[1, 4, 5] Frequently, the results are positive with production increases of 20% or more during field studies in the oil and gas industries.[1, 4] On the laboratory scale, low-frequency elastic wave stimulation has been observed to substantially increase the removal of trichloroethylene, a dense non-aqueous phase liquid (DNAPL), from a sand pack[6] and decane from sandstone[5]. On some

occasions, however, the application of low frequency elastic waves resulted in a decrease in the oil production rate in the field[1] and in the lab[5]. Suggested mechanisms for enhanced well production under seismic stimulation ("seismic" in this paper refers to all elastic stress waves in the Earth, whether their source is natural or artificial) include improved percolation of oil due to the destruction of surface films in pores[2], changes in the matrix wettability[5], shear of oil droplets due to the difference in the densities of water and oil[2], and coalescence of oil droplets due to Bjerknes forces[2]. While some or all of these mechanisms may be present in the subsurface to some extent during stimulation, they fail to include the role that mobilization of in-situ sub-pore size particles (colloids) plays in altering formation permeability. This mechanism can lead to both advantageous and disadvantageous consequences on porous mass transport, depending on whether the mobilized colloids are expelled from the system or clog the pore throats further downstream. Currently, the relative roles of the numerous physical mechanisms underlying observed changes in well production due to application of low-frequency dynamic stimulation remain to be fully determined.[1, 2, 5, 6]

The fact that seismic events can mobilize colloidal particles is evident in a study of drinking water wells after the 2001 earthquake in Nisqually, Washington.[3] As a result of this earthquake, a number of wells exhibited a marked increase in turbidity – some to the point of requiring redevelopment – as well as increases and decreases in flow.[3] Similar observations have been recorded as a result of other earthquakes in different locations.[7] Mobilization of in-situ colloids can impact more than just water turbidity. Subsurface contaminant transport may occur because natural colloidal particles can act as carriers for highly sorbing and otherwise immiscible or insoluble contaminants, such as non-aqueous phase liquids (NAPL) and actinide species.[8, 9] In addition to sorbing onto colloidal particles, NAPL droplets can also be stabilized by colloids through the formation of stable Pickering emulsions.[10] It is conceivable that elastic waves could enhance the liberation of such contaminants, resulting in either the undesirable spread of the contaminants, or the desirable recovery of the contaminants if coupled with a suitable groundwater remediation system.[8, 11] The reported enhanced liberation of colloidal particles during earthquakes is intriguing given that the natural seismic events were of a frequency lower than

expected for the release of in-situ colloidal particles.[9] As is the case for changes in well performance, the mechanisms of colloidal particle release during seismic events are still largely unknown[9], but the distribution and mobility of colloids will certainly have major impacts on mass transport in any porous system. For example, migrating fines are known to clog some pore throats of the porous networks under appropriate conditions.[9, 12] If the enhanced liberation of colloids can be understood quantitatively, then the underlying mechanisms might be utilized in developing new techniques for enhanced oil recovery and subsurface remediation.

The effects of low-frequency (30-150 Hz) acoustic stimulation on colloidal particle transport in porous media have been recently investigated[8], where the colloidal dispersion, together with a conservative tracer, was injected into a laboratory column packed with glass beads during stimulation. The results indicated that low-frequency fluid pressure stimulation did reduce the average residence time of both the colloids and the conservative tracer in the column. The reduction in the colloidal particles' residence time was independent of their size and was maximum at the lowest frequency employed (30 Hz). The study, however, did not investigate the effect of acoustic stimulation on the mobilization of previously captured colloidal particles, nor did it include mechanical stress coupled to the solid pore matrix as the dominant mode of stimulation. Other studies[6] found that the mobilization of dense NAPL (DNAPL) pools can be enhanced by low-frequency stress oscillations. Similar studies on aqueous tracers found that solute transport increased with decreasing acoustic frequency[13] and increasing acoustic intensity[14]. In previous laboratory studies[5, 6, 9, 11], low-frequency dynamic stress stimulation was observed to enhance the mobilization of NAPL and naturally occurring colloids in consolidated sandstone and unconsolidated sand. Curiously, dynamic stress stimulation not only enhanced the mobilization, but it also resulted in cyclical spikes in the effluent concentrations of both the colloids[15] and NAPL[6] when the levels of stimulation were sufficiently high. While these spikes may at first appear to be random noise, their consistent behavior and uniform timing are sufficient to believe otherwise. These cyclical spikes can provide valuable insights into the mechanisms coupling dynamic stress stimulations and mass transport in porous media, thus the mechanisms underlying enhanced oil

well production under seismic stimulation. Unfortunately, current theory fails to provide an explanation for these observed cyclical spikes or the coupling mechanisms. The work presented here has two main objectives: (1) to determine if the effluent concentration spikes are an artifact resulting from the use of natural granular materials, or if they are present when an idealized unconsolidated glass bead media is used; and (2) identify potential colloidal particle release mechanisms during low-frequency elastic wave stimulation that explain the effluent concentration behavior.

Experimental and Analytical Procedures

Column experiments were conducted using the Dynamic Core Flow Stimulation System (DCFSS)[6]. The DCFSS holds the core material in a horizontal Viton sleeve surrounded by a confining fluid. The Viton sleeve is equipped with inlet and outlet ports allowing fluids to be pumped through the core and differential pressure gauges attached to ports along the length of the sleeve to measure changes in pore fluid pressure. Static radial and axial confinement stresses were applied to the sample to simulate realistic stress conditions in the Earth and to achieve sufficient fluid seal between the core sample and the Viton sleeve. Dynamic stress stimulations with a sinusoidal waveform were induced by a mechanical actuator (Etrema Terfenol-D magnetostrictive actuator) in contact with the fluid outlet end of the packed core. The mode of stimulation was mechanical stress/strain applied directly to the solid packed beads in the axial direction, as opposed to direct coupling to the flowing pore fluid pressure.

The current experiments used an artificial porous core comprised of a 2.54-centimeter (cm) diameter by 30-cm long Teflon screen packed with 1-millimeter (mm) nominal diameter borosilicate glass beads. The sample was inserted into the DCFSS and confined at 2.4 megapascals (MPa) radial and 1.7 MPa axial static pressures. A vacuum was then applied for two days to remove as much air as possible. The core was then saturated under vacuum with de-ionized ultra-pure water at neutral pH 7 and the total pore volume was determined to be approximately 60 milliliters (mL). The core was then flushed with 18 liters (L) of the same water at a constant flow rate of 12 milliliters per hour (mL/hr), during which the permeability was determined to be 20 square microns (μm^2). Axial stress/strain measurements were acquired for the water-saturated core using a load cell in series with the mechanical actuator and a linear

variable displacement transducer (LVDT) attached to the end of the core sample. These data were used to measure Young's modulus (the ratio of stress to strain) of the bulk sample at different static and dynamic stress levels. Next, the core was injected at the same flow rate of 12 mL/hr with a 1-L suspension of 2.26-μm diameter fluorescent polystyrene (fPS) microparticles (Duke Scientific product number G0220) in ultrapure water at neutral pH 7. The number concentration of the fPS microparticles in the injected suspension was measured by flow cytometry to be approximately 1.7×10^6 particles per cm^3. The microspheres had a density of 1.05 grams per cm^3 and were negatively charged at pH 7 due to sulfate groups at the end of the polymers. The zeta (ζ) potential of the microparticles at pH 7 was measured to be -44 millivolts (mV) (Figure 1) using a Malvern Zetasizer 3000 HS. Throughout the loading process, the effluent microsphere concentration was monitored to ensure that (1) breakthrough was achieved and (2) the effluent microsphere concentration had stabilized. At the end of microsphere loading, the effluent microsphere concentration was approximately 1.1×10^6 particles per cm^3. During all experimental stages described in this paper, the flow rate through the column was maintained at 12 mL/hr, using a pulse-free pump (Quizix QX-6000) upstream of the column, resulting in an average linear velocity of 1.022 mm/minute. The core was maintained in a horizontal position throughout the experiments.

The stimulation times varied, but were on the order of hours. Although a natural seismic event would not last for such a long duration, it is common for artificial seismic sources to be applied for days or weeks during field tests where low-frequency elastic waves have been investigated for use in enhanced oil recovery. More importantly, conducting the experiment for this extended length of time allowed the temporal form of the effluent particle count curve to be determined, thereby providing valuable information about the kinetics of the particle release mechanism.

Effluent samples of 6 mL volume were collected every 30 minutes using an automatic fraction collector (Isco Foxy Junior). Samples were collected in polyethylene tubes treated with a trace amount of sodium dodecylsulfate (SDS) to minimize the coagulation of the microspheres and their deposition

onto the tube walls. The samples were capped after collection and stored at 4°C until analysis. Immediately prior to analysis, the samples were again treated with SDS and then subjected to sonication in a laboratory ultrasonic bath. These steps were determined from a set of separate experiments and found to be necessary and sufficient for the complete recovery of the microspheres in the sample tubes. Number concentrations of microspheres in the effluent samples were measured using a Partec PAS III flow cytometer. The flow cytometer was used in fluorescence mode to discriminate between the injected microspheres and any possible colloidal contaminants.

In order to gain insight into the pore-scale behavior of the microparticles, microscopic visualization experiments were conducted to confirm that the microparticles would absorb onto the surfaces of the glass beads under the conditions of column loading and to identify the likely mechanism of microparticle release as a result of dynamic stimulation. The pore-scale experiments were conducted in cells fabricated by sandwiching randomly packed 1-mm borosilicate glass beads (identical to those used in the column experiments) between two glass microscope slides (Figure 2). The cells were equipped with inlet and outlet ports, sealed with epoxy, thoroughly flushed with de-ionized ultrapure water of neutral pH 7, and then placed horizontally on the stage of an upright optical microscope. An aliquot from the same polystyrene microspheres/ultrapure water dispersion used in the core experiments was injected into the cells using a low-flow syringe pump (Harvard Apparatus Pump 33). The flow rate was adjusted to produce an average linear velocity in the cells of 1.022 mm/minute, equivalent to that used in the core experiments. Two sets of pore-scale experiments were performed. In the first, the cell was injected with just enough microsphere dispersion to completely fill the cell, the inlet and outlet of the cell were closed, and the cell was allowed to equilibrate overnight. In the second set, the microsphere dispersion was continuously injected into the cell for 17 hours, followed by continuous flushing with de-ionized ultrapure water of neutral pH 7 for 92 hours. The cell was then subjected to two different types of stimulations: (1) low-frequency oscillatory flow induced by manual actuation of the injection syringe and (2) an ultrasonic field created by an ultrasonic transducer placed on the outer surface of the cell and driven by a sinusoidal function generator and radio frequency (RF) amplifier. The purpose of the first

stimulation was to replicate the dynamic stress stimulation conditions of the core experiments and the second was to explore the effects of exciting complete sonic waves in the cell. Fluorescent images of the individual and collective glass beads were collected before, during, and after stimulation using the Automated Video Microscopic Imaging and Data Acquisition System (AVMIDAS)[16].

To interpret the results from the column experiments, the effluent particle concentration, column pressure, and confining fluid temperature data were examined using continuous wavelet transforms (CWT) to capture the presence of periodicities and waves at specific frequencies.[17] Compared to Fourier transform analysis, the CWT possesses the advantage of being able to detect waves that are transient in nature.[17] The CWT is defined as,

$$W(a,b)=\frac{1}{\sqrt{a}}\int_{-\infty}^{\infty} f(x)\psi^{*}\left(\frac{x-b}{a}\right)dx \tag{1}$$

where $W(a,b)$ is the CWT, a the scaling factor, b the position parameter, $f(x)$ the data or signal, x the independent variable of the data, and $\psi^{*}(x)$ the wavelet.[17] The scaling factor controls the size, and thus the wavelength, of the wavelet.[17] Given the discrete nature of the data reported in this paper, the CWT was implemented accordingly,

$$W(a,b)=\frac{1}{\sqrt{a}}\sum_{n=1}^{N} C_{n}\psi^{*}\left(\frac{n-b}{a}\right) \tag{2}$$

where n is the data index, N the total number of data points, and C the concentration, temperature, or pressure data. The wavelet used to analyze the data was the Haar wavelet, which is defined as,[17]

$$\psi(t)=\begin{cases} 1 \text{ for } 0 \le t < \frac{1}{2} \\ -1 \text{ for } \frac{1}{2} \le t < 1 \\ 0 \text{ otherwise} \end{cases} \tag{3}$$

Results

Core-Scale Experiments

The mechanical behavior of the saturated core is depicted in Figure 3. The behavior of the Young's modulus (stress/strain ratio) in response to dynamic stress shows a marked change in the 100 to 150

kilopascals (kPa) RMS stress amplitude range. This observation indicates a threshold-type behavior where a change in the nonlinear stress/strain response of the bead pack occurs above certain stress amplitudes.

The normalized particle breakthrough curves, $C/C_o(t)$, and associated continuous wavelet transforms (CWT) for the three dynamic stress stimulation episodes are shown in Figures 4 through 6. In these figures, $C(t)$ is the effluent microparticle number concentration at any given time, t, and C_o is the effluent microsphere concentration prior to stimulation, which was calculated by averaging about 20 effluent samples prior to stimulation and found to be approximately 292, 194, and 142 cm^{-3} for the first, second and third stimulation episodes respectively. Also provided are the fractions of remaining particles released from the column, determined by mass balance calculations of cumulative numbers of particles injected and released from the column prior to the start of each stimulation episode.

Figure 4 shows the results of the first dynamic stress stimulation episode (90.5 hr duration; 26 Hz frequency; 200 kPa RMS stress amplitude). At the start of stimulation, $C/C_o(t)$ spiked at 7.4 before dropping and spiking again to approximately 11.75. These two spikes are manifested in the CWT as distinctive *V*-shaped features. The width of the first spike is 5 samples (150 minutes). Because of its range, this spike is believed to be due to an actual concentration spike in the collected samples. Random noise (e.g., an isolated miscounting of a sample by the flow cytometer, or a contaminated sample) would have a range of only one sample. Also, the samples were analyzed in random order as determined by a random number generator in a spreadsheet. As a result, longer term errors introduced by instrument drift would appear in the data as discontinuities with ranges of 1 or 2 samples. After the second spike, $C/C_o(t)$ decays exponentially – consistent with first-order release kinetics. A few spikes in $C/C_o(t)$ are also observed during this exponential decay. However, these few spikes are weak and infrequent, and do not appear to occur at any regular interval that would suggest cyclic behavior. $C/C_o(t)$ continued to decay after stimulation ceased, reaching a stabilized value of approximated 0.53. The column pressure was observed to cycle through a 24-hour pattern that closely matched the background temperature variations measured in the column and the laboratory room. Thus, these apparent pressure cycles were caused by

room temperature influencing the gain of the pressure transducers. Any actual pressure changes in the column due to stimulation were below the level of detection during this first episode.

Figure 5 shows the results of the second dynamic stress stimulation episode (5.5 hr duration; 26 Hz frequency; 350 kPa RMS stress amplitude). During stimulation the effluent microsphere concentration demonstrated an increasing trend, occurring in three distinct spikes, to a maximum value of approximately 140 C_o immediately prior to the end of stimulation. This maximum value is more than one order of magnitude higher than the maximum $C/C_o(t)$ value observed in the previous episode and is due to the higher RMS stress amplitude applied. As before, the range of each spike seen in this episode is on the order of 4 to 5 samples (120 to 150 minutes) and the presence of the spikes is noted by three distinctive *V*-shaped features in the CWT. At the end of the stimulation, the concentration dropped to approximately 0.73 C_o. No additional effluent concentration spikes – outside of random noise – are observed in the data. Likewise, there are no additional *V*-shaped features present in the CWT. As was observed during the first episode, the pressure data correlated strongly with the room temperature data, and any actual pressure changes in the column due to stimulation were below the level of detection.

Figure 6 shows the results of the third dynamic stress stimulation episode, where the applied RMS stress amplitude was the same (350 kPa) as in the second episode but the duration was increased to 25.5 hours. Shortly after the start of stimulation, the effluent concentration increased to a maximum of approximately 63 C_o and then followed an exponentially decaying trend throughout the remainder stimulation. Superimposed on the exponential decay are a series of distinct concentration spikes separated by an average interval of 5.875 samples (176 minutes), visible as a series of *V*-shaped features in the CWT. Surprisingly, these spikes continued to occur, but with diminished intensity, at regular intervals for 78 samples (39 hours) after stimulation was stopped. They then dampened out as the effluent concentration stabilized at approximately 0.85 C_o. Concentration spikes were not observed before stimulation was applied.

Figure 7 shows the temperature and pressure data along with the associated CWTs for the third episode. The data in this figure have been normalized using the following equations,

$$P_{normalized} = \frac{P - P_{min}}{P_{max} - P_{min}} \quad (4)$$

$$T_{normalized} = \frac{T - T_{min}}{T_{max} - T_{min}} \quad (5)$$

where P_{min} = -2.59 kPa, P_{max} = -0.412 kPa, T_{min} = 22.3°C, and T_{max} = 29.5 °C are the minimum and maximum pressures and temperatures, respectively, observed over the entire time span of the stimulation experiments. Notice that prior to stimulation the pressure data correlate strongly with the background temperature data. Both data sets display the same 24-hour pattern observed during the previous two stimulation episodes. Thus, the pressure data fluctuations prior to stimulation are again due to temperature-induced transducer gain variations and do not represent actual pressure changes within the column. During stimulation, however, the pressure fluctuations begin to significantly deviate from the behavior of the temperature data. This loss of correlation was not observed in the previous two episodes and indicates the appearance of actual pressure changes within the column. Initially, the 24-hour pressure pattern becomes unstable (at about t = 300 minutes). By the time stimulation is stopped, the pressure and temperature data are completely uncorrelated. This persists until around t = 3000 minutes, at which point the original 24-hour correlation cycle is restored. The onset of pressure instability, loss of correlation and recovery to background conditions can all be seen clearly in the pressure and temperature CWTs. The pressure data CWT demonstrates that the instabilities occur with approximately the same periodicity as the $C/C_0(t)$ spikes seen in Figure 6 and cease at approximately the same time.

Pore-Scale Experiments

In the initial pore-scale experiment, where the fPS microparticles dispersed in ultrapure water were allowed to equilibrate in the absence of flow, the microspheres were observed to settle to the bottom of the cell without adsorbing onto the surface of the glass beads. At first, the microspheres were uniformly distributed throughout the cell and exhibited random thermal motion. Overnight the microspheres

settled and adsorbed onto the cell's bottom surface and no microspheres were observed to adsorb onto the surface of the glass beads.

In the subsequent pore-scale experiment, where the microparticle dispersion was continuously injected through the cell, a significant number of microparticles adsorbed onto the surfaces of the glass beads and the cell's bottom surface. Continuous flushing with ultrapure water at the same flow rate as that of injection did not cause any observable changes in the beads' surface coverage. The microparticles coated the glass beads and the degree of coverage decreased from the inlet to the outlet, indicating that more sites on the beads' surfaces were still available for adsorption in the cell's outlet region. While continuing experiments prevented the disassembly of the packed beads column and inspection of the beads, the results of the second pore-scale episode indicate that the microspheres adsorbed onto the glass beads in the column, where loading occurred under continuous flow. Given that both the microparticles and glass beads are negatively charged under the current chemical conditions (de-ionized water, pH ~7), the above pore-scale observations manifest the increased collision efficiency between the microparticles and the beads caused by flow through the cell, resulting in significant microparticle adsorption onto the surface of the beads.

Low-frequency flow oscillations caused the glass beads to shift and rotate, rubbing their surfaces together. Evidence of microparticle scraping and displacement on the beads' surfaces when beads rub against each other is given in Figure 8, and when beads rub against the cell walls in Figure 9. In Figure 8, a distinctive patch at location "1" in the top image is observed to move to location "2" in the bottom image. The inset highlights a path scraped clear of microspheres by rubbing against a neighboring bead, where location "3" in the inset is the approximate point of contact when the bottom image was captured. In Figure 9, the scraping of the bead against the cell wall is observed to generate two piles of microparticles in front of the point of contact. The inset in the top image highlights the areas cleared of microparticles by the contact; as does the inset in the bottom image, where the wide, blue marks indicate two new areas cleared of microparticles during the capturing of the top and bottom images.

Finally, acoustic stimulation of the pore scale cell at different ultrasonic frequencies did not cause scraping of the adsorbed microparticles and the grinding of beads against each other or the cell walls was not observed. The ultrasonic stimulations were only able to move some beads that were not in tight contact with their neighbors or the cell walls, causing them to hit their neighboring beads and the top and bottom surfaces of the cell.

Discussion

The core-scale experiments demonstrate that low-frequency stimulation mobilizes captured microparticles whose diameters are much less than the wavelength of stimulation. The microparticle effluent concentration behavior during stimulation points to at least two distinct microparticle release mechanisms. One release mechanism is responsible for the uniform exponential decay in $C(t)$ and another is responsible for the distinct spikes at higher stress amplitude. The sudden drop in the exponential decay behavior of $C/C_0(t)$ shortly after ceasing stimulations depicted in Figures 4 and 6 indicates that the first mechanism operates only during stimulations. The continuation of concentrations spikes after ceasing stimulations in Figure 6, on the other hand, indicates that the second mechanism operates during and after the dynamic stress stimulations. The exponential decay is attributed to a first-order release kinetics of the microparticles from the glass beads surfaces that is relatively uniform throughout the bead pack.[15] The pore scale experimental observations (Figures 8 and 9) suggest that this relatively uniform microparticle release is due to the localized grinding of the beads that is expected to take place among the majority of the beads throughout the pack. The distinct concentration spikes, on the other hand, can be attributed to simultaneous rearrangements of multiple grains producing discrete, en masse releases of adsorbed microparticles. These simultaneous rearrangements can be explained by the formation of "circulation cells" that consist of multiple grains rotating as a rigid mass during compaction of the bead pack. These circulation cells have been documented in the literature[18] to take place in granular material and are evident by our preliminary discrete element modeling (DEM)[19] results shown in Figure 10. It has been suggested that these cells develop due to buckling of the particle force chains.[18]

The abrupt incidents of circulation cells in the packed bead column resulting in a discrete, en masse release of particles is consistent with the erratic pressure data coinciding with the discrete microparticle releases during the third stimulation episode (Figures 6 and 7). If these circulation cells occur during stimulation, in other words during compaction of the glass bead pack, it can be argued that they are also likely present during post-stimulation, in other words during the slow relaxation of the compacted bead pack. Thus, the presence of circulation cells can explain the continued discrete microparticle release after stimulation. Additional evidence of these circulation cells stems from the observed sudden change in the Young's modulus behavior in Figure 3. This sudden change is likely associated with the activation of a new mechanical interaction mechanism between individual beads, which can in turn be attributed to the development of circulation cells within the column. Figure 3 indicates that the activation of this mechanism occurs above a given stress amplitude threshold in the 100 to 150 kPa range. However, the discrete, en masse release of particles was only distinguishable during the core-scale column experiments at stress amplitudes above 200 kPa. This small discrepancy can be explained by the fact that, as indicated by axial column length data, the column was more compact during the stimulation episodes reported here than during the initial stress/strain data collection. We expect that column compaction increases the Young's modulus and, hence, the stress amplitude required to initiate circulation cells.

Identical behavior of distinct spikes in column effluent concentrations, thus the en masse releases, was observed for naturally occurring colloids[15] and NAPL[6] during and after low-frequency dynamic stress stimulations of sandstone and irregularly-shaped natural sand, respectively. As a result, the behavior of the column in the current experiments cannot be attributed to the idealized shape of the current packing, or to its non-cohesive nature. Circulation cells are not anticipated in cohesive materials such as sandstone. However, microfracturing due to transgranular and intergranular fractures, as well as grain deformation, sliding, and rotation mechanisms that have been documented in the literature[20, 21] to occur during stressing and compaction weakening of sandstone and appear likely to produce similar

effects and result in discrete, en masse releases of adsorbed microparticles or NAPL in these systems. Further research is planned to confirm the presence of these mechanisms.

Modeling

To simulate the column effluent concentration behavior during the second and third stimulation episodes (Figures 5 and 6), the overall behavior was broken down into those behaviors expected from the two mechanisms discussed above. The first mechanism, i.e., first-order microparticle release kinetics, can be described by the simple exponential decay function:

$$P1_n = a\exp(-b \cdot n) \tag{7}$$

where n is the sample number, $P1_n$ is the total microparticle count contained in sample n due to the localized grinding release mechanism, and a and b are constants representing the initial jump in microparticles concentration and the decay rate constant, respectively. Equation 7 was fit to the data minima between the concentration spikes in Figure 6, resulting in values of a = 2969.5 and b = 0.035. Prior to sample number 5 (the maximum of the first data spike), $P1_n$ was assumed to be zero.

The total particle count due to the discrete, en masse releases ($P2_n$) was then added to $P1_n$. $P2_n$ was assumed to be zero everywhere except for sample numbers that coincide with actual and apparent spike maxima in Figure 6 (n = 5, 8, 12, 16, 18, 23, 25, 28, 32, 37, 39, 45, and 47). To simulate the advective-diffusive transport of the microparticles in the column, the summation was then convolved with a Gaussian function:

$$TP_n = \frac{1}{N}\sum_{i=-5}^{5}\left\{\left(P1_{n+i} + P2_{n+i}\right)\cdot \exp\left[\frac{-\left(i^2\right)}{\lambda}\right]\right\} \tag{8}$$

where TP_n is the total particle count in sample n, N is a normalization constant, and λ controls the width of the Gaussian function. N was determined accordingly:

$$N = \sum_{i=-5}^{5}\exp\left[\frac{-\left(i^2\right)}{\lambda}\right] \tag{8}$$

Fitting the model to the data required determining the values for λ and $P2_n$. Using a simple Monte Carlo algorithm coded in FORTRAN that minimized the root mean squared error between the

experimental data and the model, it was determined that $\lambda = 1.66$ and $P2_n$ = 6568, 5633, 758, 3858, 1233, 2588, 1003, 1277, 6600, 957, 2797, 243, and 460 at n = 5, 8, 12, 16, 18, 23, 25, 28, 32, 37, 39, 45, and 47, respectively. The top graph in Figure 11 provides the experimental data from the third episode during stimulation expressed in terms of total particles per sample, along with the exponential curve fit to the data minima and the modeled concentration spikes ($P1_n + P2_n$). The bottom graph compares the convolved model (TP_n) with the experimental data. The Pearson product moment correlation coefficient between the data and the convoluted model equals 0.952, indicating an excellent agreement of the simulations with the experimental data.

Conclusions

Low-frequency mechanical stimulation of a glass bead packed column mobilized adsorbed microparticles whose diameters are orders of magnitude less than the wavelength of stimulation. The most plausible release mechanisms appear to be associated with the compaction and relaxation of the granular material that result in the scraping of the grain surfaces, thereby mechanically displacing the adsorbed microparticles. The results of past studies suggest that similar compaction/surface scraping-based mechanisms are also present in natural granular and cohesive materials. While further research is needed to confirm the presence of these mechanisms, this study supports the hypothesis that the changes in oil and water well production often observed during and after seismic events may be due, in part, to the release of natural colloids. This can cause either beneficial or harmful effects on formation permeability, depending on whether the released particles are expelled from the porous matrix or cause subsequent downstream fouling of flow pathways. The results of this study appear to indicate that any event resulting in the compaction of an oil-bearing formation – seismic or otherwise, including a reduction in pore pressure due to oil recovery – may reduce the production rate if the formation has a low permeability and a high natural colloids concentration.

Acknowledgments

This work was funded by the U.S. Department of Energy Basic Energy Sciences Program under the Los Alamos National Laboratory contract no. DE-AC52-06NA25396. This manuscript has been approved for public distribution by Los Alamos National Laboratory under LA-UR-xx-xxxx.

References

[1] Roberts, P.M., I.B. Esipov, and E.L. Majer, "Elastic Wave Stimulation of Oil Reservoirs: Promising Eor Technology?," The Leading Edge, **22**(5): p. 448-453 (2003).

[2] Beresnev, I.A. and P.A. Johnson, "Elastic-Wave Stimulation of Oil Production: A Review of Methods and Results," Geophysics, **59**: p. 1000-1017 (1994).

[3] Ballantyne, D. and W. Heubach, "Water Supply,' in *The Nisqually, Washington, Earthquake of February 28, 2001*, P.W. McDonough, Editor. 2002, ASCE Publications: Reston, VA.

[4] Kostrov, S.A., W.O. Wooden, and P.M. Roberts, "In Situ Seismic Shockwaves Stimulate Oil Production," Oil and Gas Journal, **99**(36): p. 47-52 (2001).

[5] Roberts, P.M., E.L. Majer, W.-C. Lo, G. Sposito, and T.M. Daley, "An Integrated Approach to Seismic Stimulation of Oil Reservoirs: Laboratory, Field and Theoretical Results from Doe/Industry Collaborations," in *Nonlinear Acoustics at the Beginning of the 21st Century*: Faculty of Physics, MSU (2002).

[6] Roberts, P.M., A. Sharma, V. Uddameri, M. Monagle, D.E. Dale, and L.K. Steck, "Enhanced Dnapl Transport in a Sand Core During Dynamic Stress Stimulation," Environmental Engineering Science, **18**(2): p. 67-79 (2001).

[7] Elkhoury, J.E., E.E. Brodsky, and D.C. Agnew, "Seismic Waves Increase Permeability," Nature, **441**(7097): p. 1135-1138 (2006).

[8] Thomas, J.M. and C.V. Chrysikopoulos, "Experimental Investigation of Acoustically Enhanced Colloid Transport in Water-Saturated Packed Columns," Journal of Colloid and Interface Science, **308**: p. 200-207 (2007).

[9] Roberts, P.M., "Laboratory Observations of Altered Porous Fluid-Flow Behavior in Berea Sandstone Induced by Low-Frequency Dynamic Stress Stimulation," Acoustical Physics, **51**(Suppl. 1): p. S140-S148 (2005).

[10] Tarimala, S. and L.L. Dai, "Structure of Microparticles in Solid-Stablized Emulsions," Langmuir, **20**(9): p. 2492-3494 (2004).

[11] Roberts, P.M. and A.I. Abdel-Fattah, "Low-Frequency Dynamic-Stress Effects on Core-Scale Porous Fluid Flow Due to Coupling with Sub-Pore-Scale Particle Interactions," in *Innovations in Nonlinear Acoustics: 17th International Symposium on Nonlinear Acoustics*: American Institute of Physics (2006).

[12] Santamarina, J.C., J.R. Valdes, A.M. Palmino, and J. Alvarellos, "Viscous Effects in Particulates," in *IUTAM Proceedings on Physicochemical and Electromechanical Interactions in Porous Media*: Springer (2005).

[13] Vogler, E.T. and C.V. Chrysikopoulos, "Experimental Investigation of Acoustiaclly Enhanced Solute Transport in Porous Media," Geophysical Review Letters, **29**(15): p. 5-1 to 5-4 (2002).

[14] Cherskiy, N.V., V.P. Tsarev, V.M. Konovalov, and O.L. Kuznetsov, "The Effect of Ultrasound on Permeability of Rocks to Water," Transact. USSR Acad. Sci., Earth Sci. Sect., **232**: p. 201-204 (1977).

[15] Roberts, P.M. and A.I. Abdel-Fattah, "Seismic Stress Stimulation Mobilizes Colloids Trapped in a Porous Rock," Earth and Planetary Science Letters, **284**: p. 538-543 (2009).

[16] Abdel-Fattah, A.I. and P.M. Roberts, "Microscopic Behavior of Colloidal Particles under the Effect of Acoustic Stimulations in the Ultrasonic to Megasonic Range," in *Innovations in*

Nonlinear Acoustics: 17th International Symposium on Nonlinear Acoustics: American Institute of Physics (2006).

[17] Stark, H.-G., "Wavelets and Signal Processing, an Application-Based Introduction." 2005, The Netherlands: Springer.

[18] Rege, N.V., *Computational Modeling of Granular Materials*, in *Department of Civil and Environmental Engineering*. 1996, Massachusetts Institute of Technology: Cambridge, MA. p. 152.

[19] Cundall, P.A. and O.D.L. Strack, "Discrete Numerical Model for Granular Assemblies," Geotechnique, **29**(1): p. 47-65 (1979).

[20] Sayers, C.M. and P.M.T.M. Schutjens, "An Introduction to Reservoir Geomechanics," The Leading Edge, **5**: p. 597-601 (2007).

[21] Schutjens, P.M.T.M. and H.d. Ruig, "The Influence of Stress Path on Compressibility and Permeability of an Overpressured Reservoir Sandstone: Some Experimental Data," Physics and Chemistry of the Earth, **22**(1-2): p. 97-103 (1997).

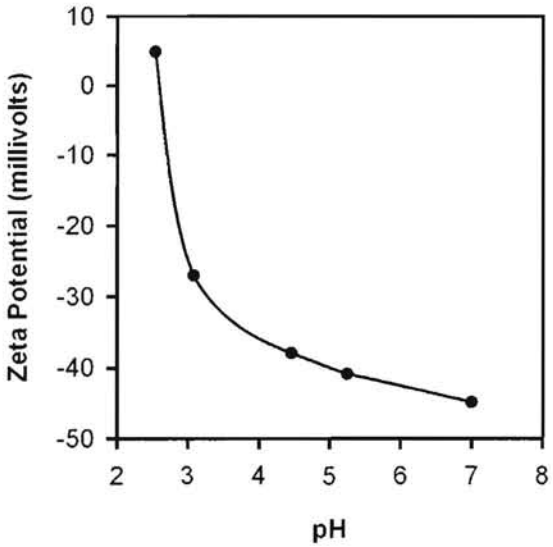

Figure 1. Zeta potential of 2.26 μm fluorescent polystyrene microspheres (Duke Scientific product number G0220) in water at varying pH levels as measured on a Malvern Zetasizer 3000 HS.

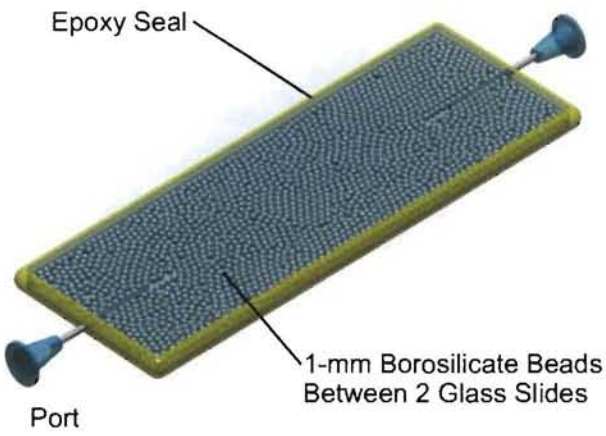

Figure 2. Rendering of the pore scale experimental cell design.

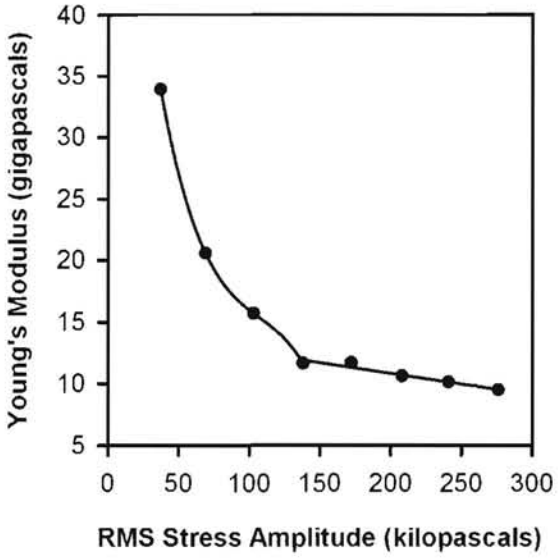

Figure 3. Young's modulus data for the flooded glass bead pack in the DCFSS column prior to loading with colloidal particles.

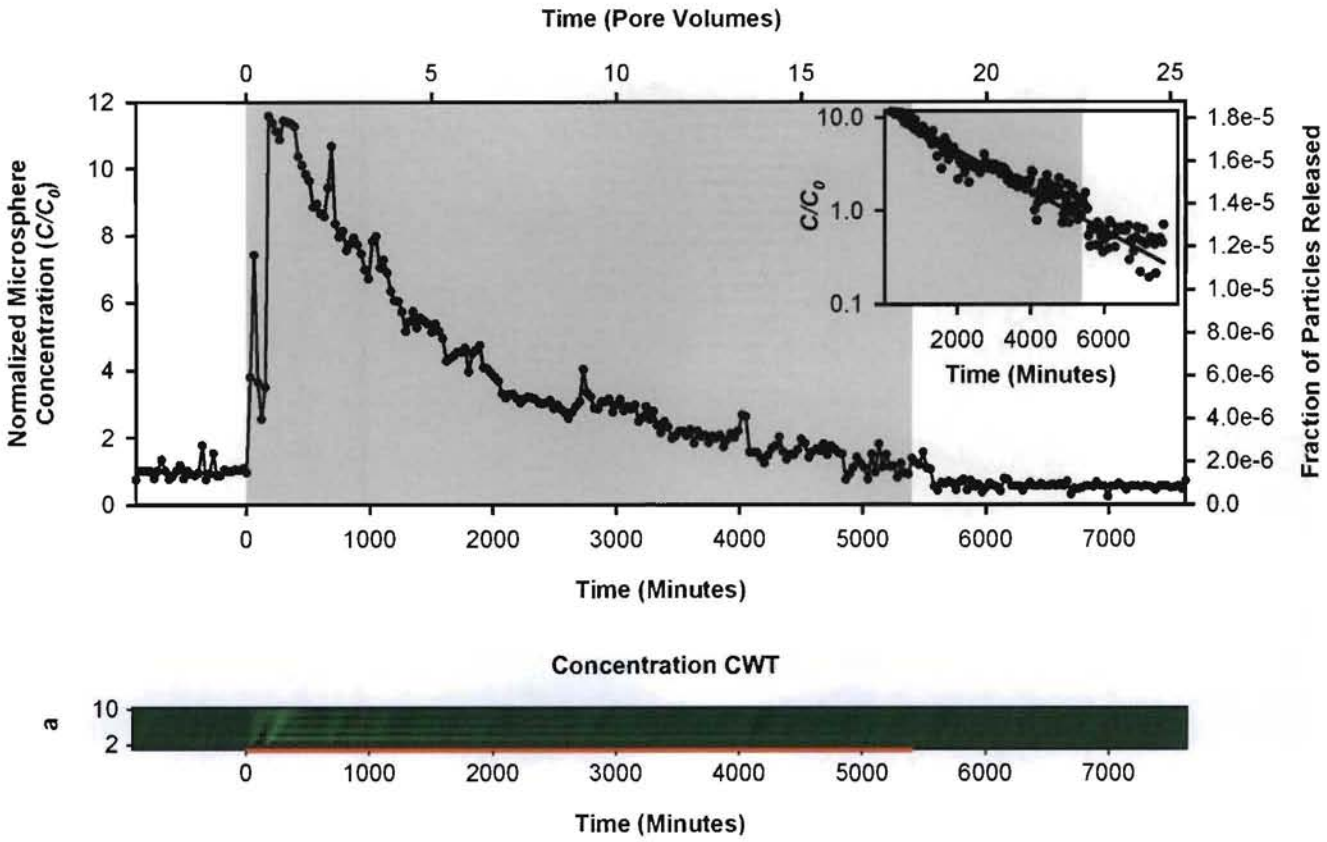

Figure 4. Normalized effluent microsphere concentration data (top, dot-line) and wavelet transform (bottom) for the first dynamic stress stimulation episode at 26 Hz frequency and 200 kPa amplitude. Time (t) = 0, shaded background, and red horizontal line indicate the start of stimulation and its duration. The concentration data are also plotted on a semi-logarithmic scale (inset, dot) from the start of stimulation, with an exponential decay curve (inset, line) fit to the data by root mean squared error minimization.

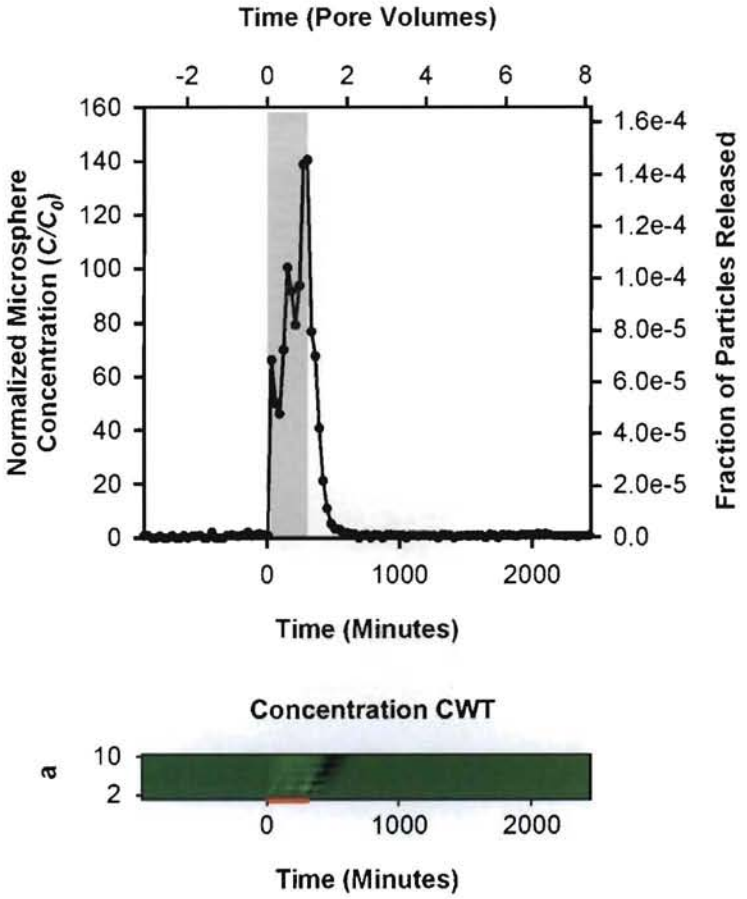

Figure 5. Normalized effluent microsphere concentration data (top, dot-line) and wavelet transform (bottom) for the second dynamic stress stimulation episode at 26 Hz frequency and 350 kPa amplitude. Time (t) = 0, shaded background, and red horizontal line indicate the start of stimulation and its duration.

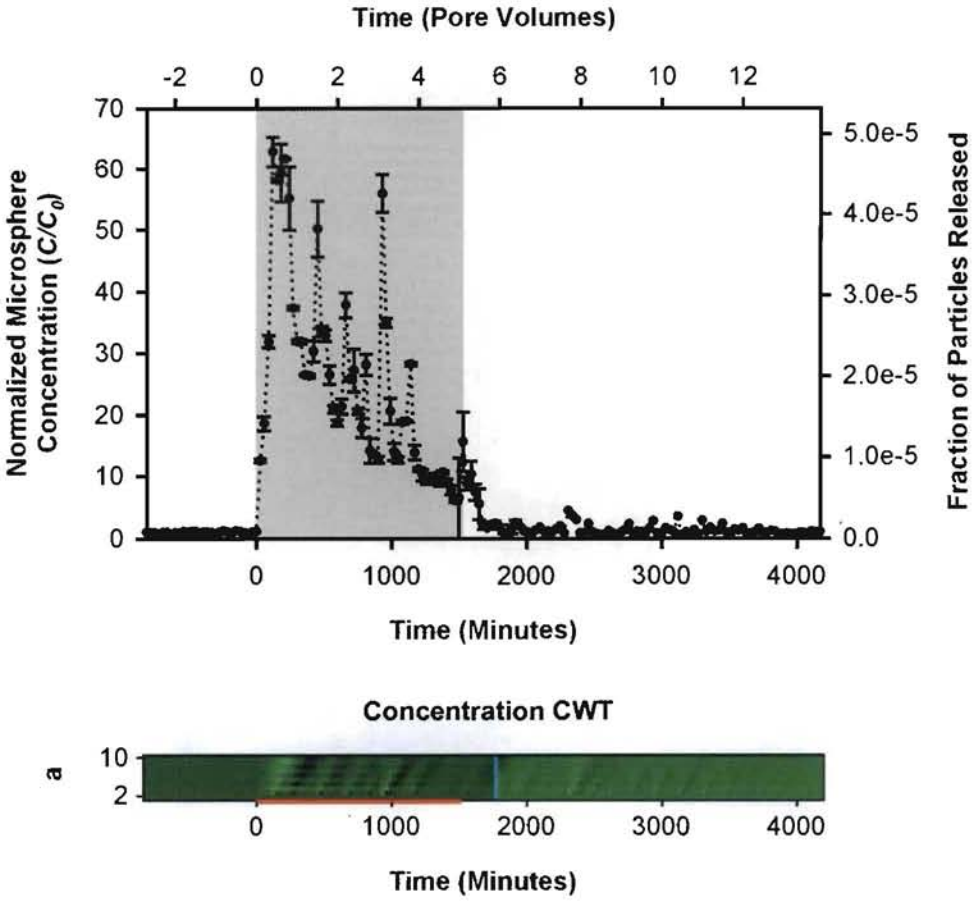

Figure 6. Normalized effluent microsphere concentration data points and averages with error bars (top) and wavelet transform (bottom) for the third dynamic stress stimulation episode at 26 Hz frequency and 350 kPa amplitude. Time (t) = 0, shaded background, and red horizontal line indicate the start of stimulation and its duration. The contrast and brightness of the CWT is enhanced to the right of the blue line.

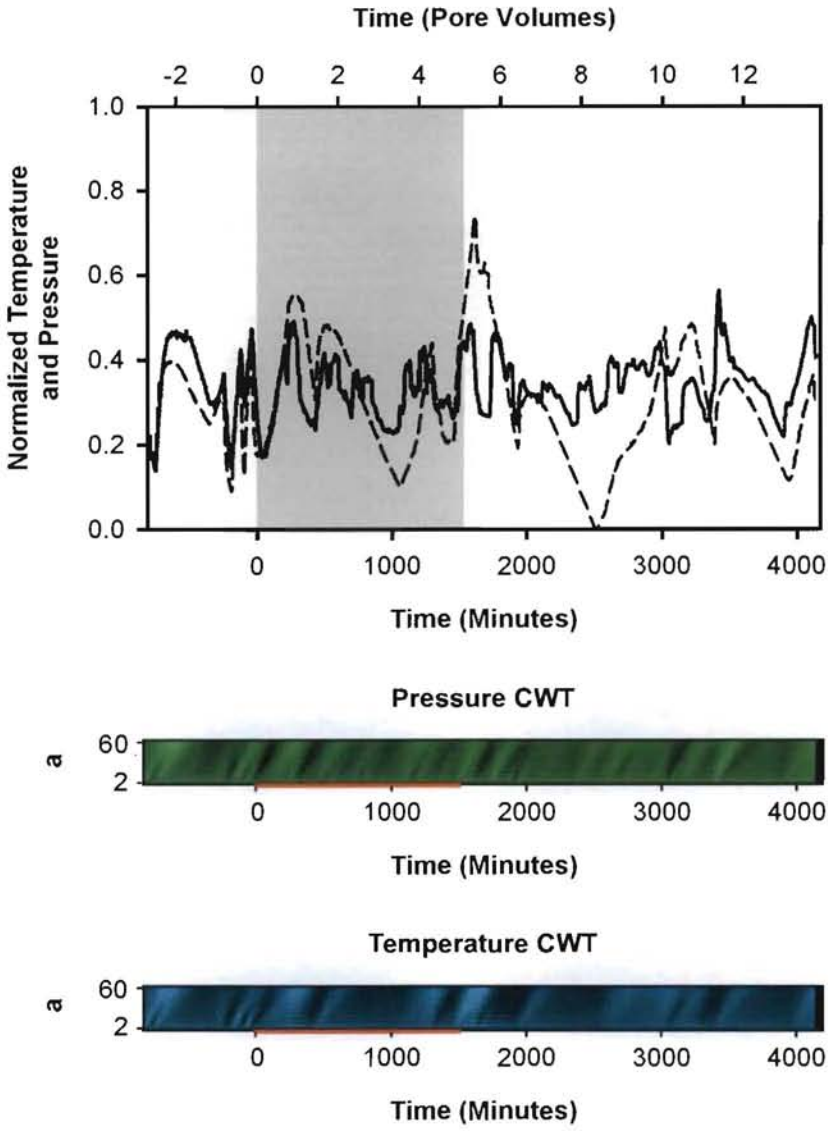

Figure 7. Normalized column pressure data (top, solid line), confining vessel internal temperature (top, dashed line), and corresponding CWTs for the third dynamic stress stimulation episode at 26 Hz frequency and 350 kPa amplitude. Time (t) = 0, shaded background, and red horizontal line indicate the start of stimulation and its duration.

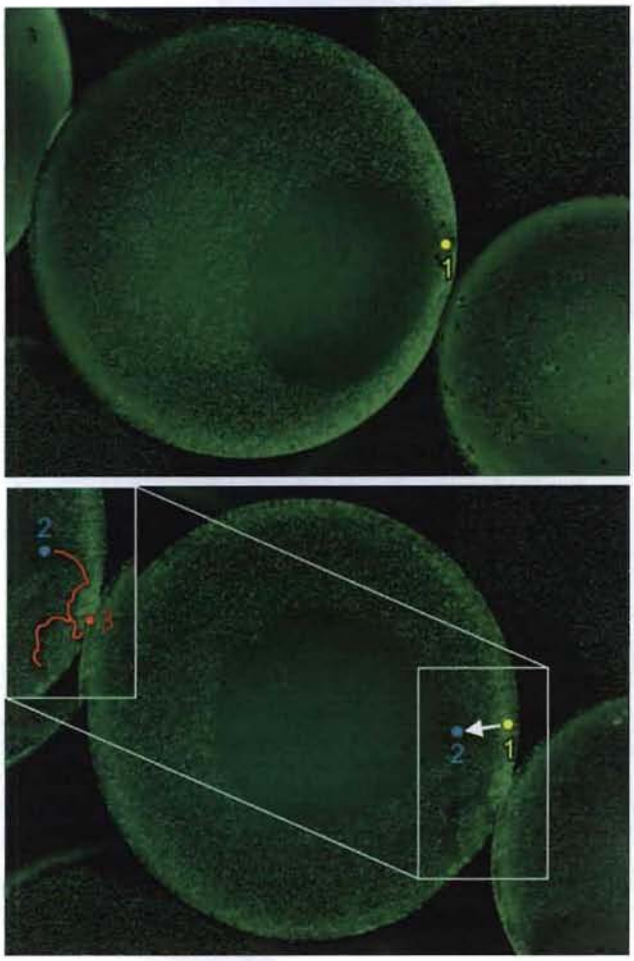

Figure 8. Fluorescent images captured at 50X magnification of glass beads coated with fPS microspheres after continuous loading followed by flushing with ultrapure water. Images captured before (top) and after (bottom) an episode of low-frequency flow oscillations. A distinctive patch at location "1" in the top image rotates to location "2" in the bottom image. The inset highlights a path on the surface of the bead scraped clean by contact during rotation with a neighboring bead. Location "3" in the inset is the approximate point of contact when the bottom image was captured.

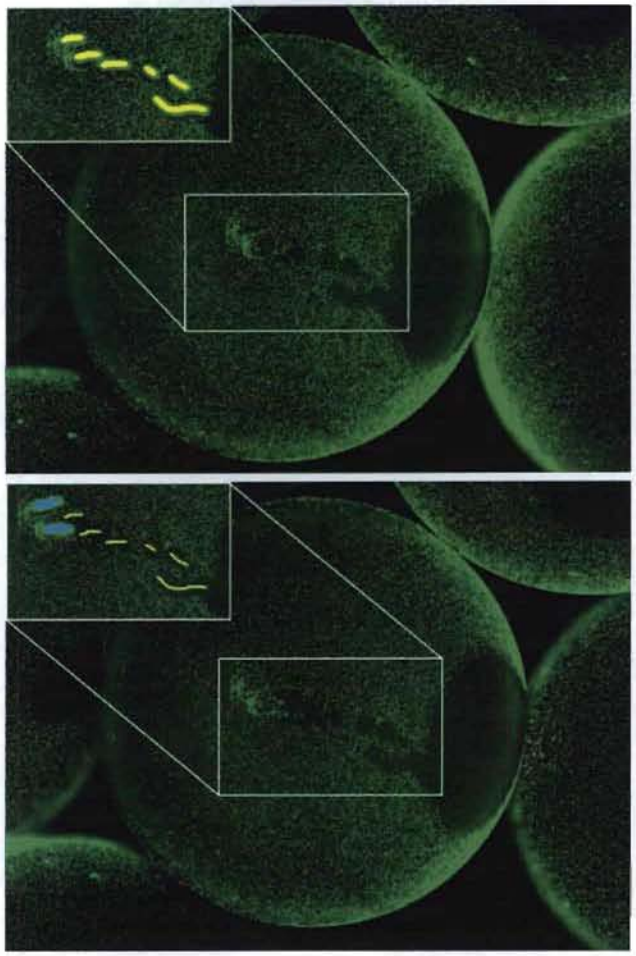

Figure 9. Fluorescent images captured at 50X magnification of glass beads coated with fPS microspheres after continuous loading followed by flushing with ultrapure water. Images captured before (top) and after (bottom) an episode of low-frequency flow oscillations. These two images provide evidence of the beads scraping against the cell wall during oscillations, as well as the piling up of particles in front of the point of contact. The insets highlight the locations of the paths scraped clear, with the yellow marks indicating areas scraped before the top image was captured, and blue marks in the bottom image showing new areas scraped after the top image was captured.

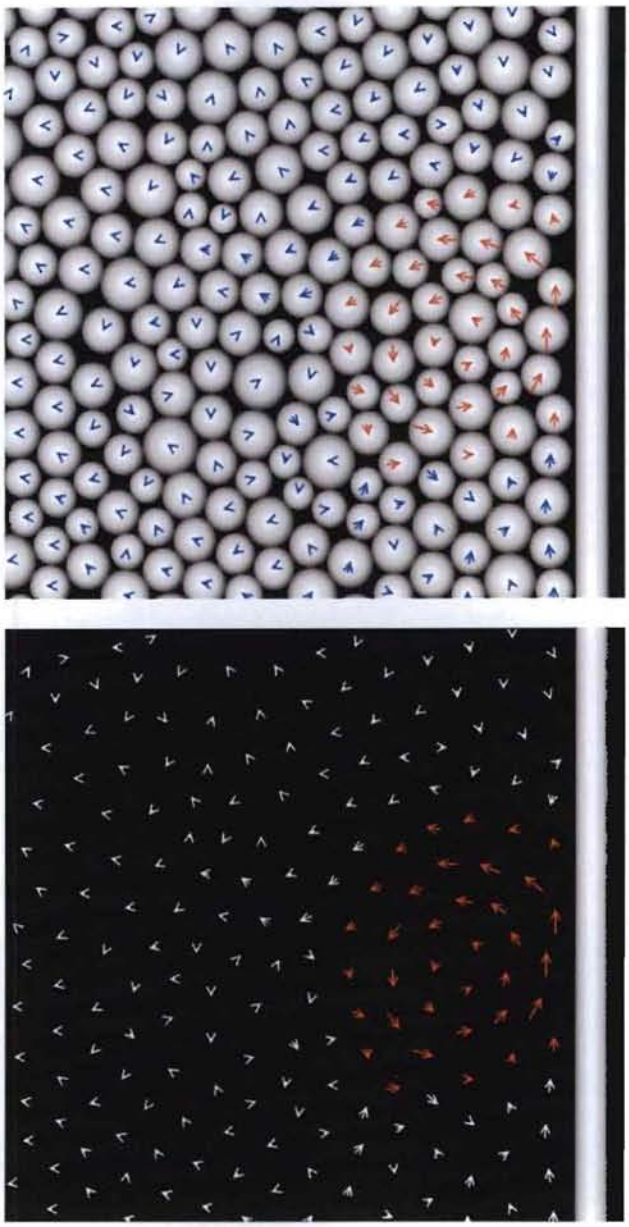

Figure 10. Preliminary Discrete Element Model results of a confined, polydisperse granular material under compaction, illustrating the presence of a "circulation cell." The arrowheads indicate the grains' direction of travel over several thousand time steps and the arrow tails plot the initial and final positions of the grains over the time span of interest. The arrows are superimposed onto the grains in their final positions (top) to illustrate the grains' relative diameters and provided without the grains (bottom) for clarity. The circulation cell is indicated by the use of red arrows.

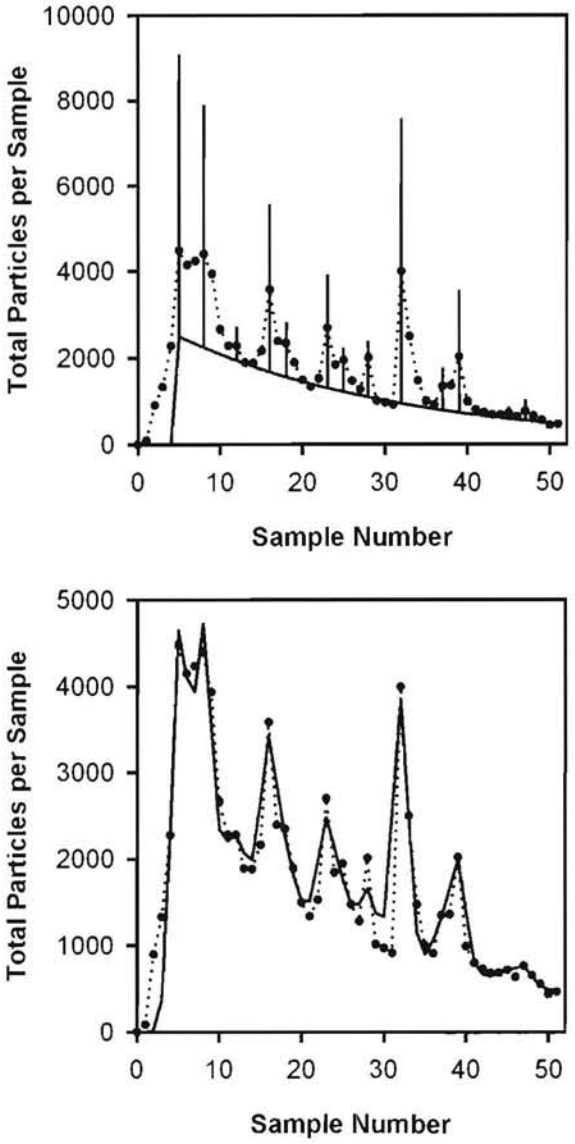

Figure 11. Comparison of experimental data and model. The data from the third stimulation episode (top and bottom, points and dotted line) can be modeled by an exponential decay fit to the data minima plus discrete concentration spikes (top, solid lines). Convolving the decay and spikes with a Gaussian function to simulate diffusion and multiple flow pathways within the column (bottom, solid line) provides a good fit between the simulation results and experimental data.

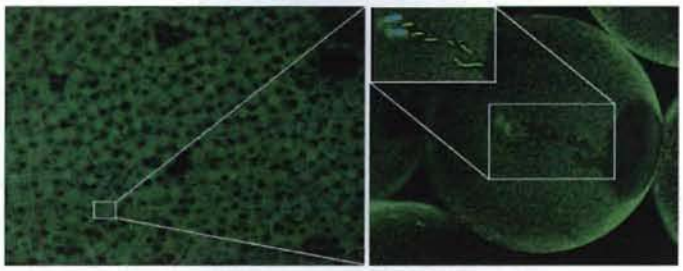

Table of Contents Figure.

Dr. Chatfield,

We appreciate the opportunity to submit a revised manuscript. Many of the reviewers' comments were very constructive and the manuscript has been significantly rewritten based on the feedback provided. Attached, we describe how the revised manuscript addresses each comment. If you or the reviewers have any additional questions or concerns, please feel free to contact us at your convenience.

Sincerely,

Dr. Amr Abdel-Fattah

The manuscript concerns the release of polystyrene colloids from glass bead porous media via elastic wave stimulation. Low frequency stimulations of various intensities and durations produced cyclical variations in column effluent colloid concentrations, and for long stimulation durations these cyclical variations coincided with fluctuations in the column pressures. Microscopy verified that colloid release resulted from glass bead rotation during stimulation.

It is not clear to this reviewer whether the subject of this article is of interest to readers of Langmuir. It seems to this reader that the manuscript is better suited to geophysical journals such as J. Geophys. Research, or Water Resources Research. Regardless of suitability, the manuscript can be strengthened in some respects detailed below before it is published.

1) The introduction does not prepare the reader to comprehend the significance of the results shown in figures 3-8.

The manuscript has been revised to emphasize the significance of the results. Specifically: (1) we demonstrate the ability of low-frequency elastic wave stimulation to mobilize colloids; (2) our data indicate the kinetics of the release mechanisms; (3) we propose feasible release mechanisms consistent with release kinetics and microscopic observations; and (4) explain the potential for low-frequency elastic wave stimulation to reduce oil well production - an explanation missing from the current theory.

No background is provided to link the pressure temperature fluctuations to the low frequency stimulation.

There appears to be a great deal of confusion on the part of both reviewers regarding this particular topic. We do not believe that there exists a link between the pressure/temperature fluctuations and the low-frequency stimulation. Recognizing that our previous manuscript led both reviewers to the opposite conclusion, we have revised our manuscript clarify that: (1) the column temperature fluctuations are only due to the 24-hour temperature fluctuations in the lab housing the column; (2) the 24-hour pressure fluctuations are due to the 24-hour temperature fluctuations impacting the gain of the pressure sensors and do not indicate actual pressure fluctuations within the column; and (3) the pressure data should be applied to the column only when there is <u>not</u> a link between the temperature and pressure.

How exactly does the stimulation lead to these pressure and temperature fluctuations?

We do not believe that there exists a link between the pressure/temperature fluctuations and the low-frequency stimulation. The manuscript has been revised to clarify this point.

What is the significance of the 24-hour cycles?

The significance of the 24-hour cycles is: (1) they make it clear that most of the pressure fluctuations are due environmental factors and not actual pressure changes within the column and (2) only the pressure data that does not follow a 24-hour cycle can be interpreted as representative of the column's pressure. The manuscript has been revised to further clarify these points.

Furthermore, in the results section of the paper these questions are not answered.

We believe that these questions have arisen due to a misunderstanding of the true point we were attempting to make in the manuscript. As such, we have revised the manuscript to better emphasize that there exists no link between the 24-hour temperature/pressure fluctuations and the low-frequency stimulation.

What does it mean when the pressure and temperature become uncoupled?

It means that the pressure is no longer linked to the 24-hour environmental temperature cycle and thus should be considered as indicative of the actual pressure behavior within the column. Of particular importance is the fact that the pressure decouples from the temperature cycle and becomes erratic only during higher stress amplitudes and correlates with the discrete, en masse releases of microparticles. Thus, any proposed mechanism for the discrete, en masse releases should predict erratic pressure data (e.g., the development of rotational cells). The manuscript has been revised to emphasize this meaning.

The manuscript raises many questions in this regard that are not answered in the results or discussion. As a result, the reader feels as if they are in a guessing game regarding the significance of the results for Figures 3-8.

We hope that our revisions to the manuscript no longer leave readers with the impression that they are in a guessing game.

2) For figures 9-10 the reader is also left wondering what the significance of the observation is. For example, it appears that the point of the discussion of figure 9 (top) on the top of page 11 is that the microspheres did not attach to the glass beads. Is that correct?

That statement is 50% correct. Depending on the conditions of microparticle loading, the microparticles may or may not attach to the glass spheres. This point is of critical importance. Keep in mind that our system consists of negatively charged microparticles, negatively charged glass beads, and deionized water. It should not be concluded a priori that the microparticles injected into

the column adsorbed onto glass beads. On the contrary, DLVO theory predicts the opposite - as was observed during the first flowcell experiment. Fortunately, the conditions used for column loading also resulted in microparticle capture.

Likewise, for figure 9 (bottom), as well as figure 10, the conclusions here are not made clear. In fact this section seems solely to be preparative for the optical observations made in figures 11-14. If that is in fact the goal of this section, then the number of figures (3-10) and text devoted is far too much for what is needed to make the points in this first section of the paper. There are too many figures and sections that leave the reader wondering: "is this unexpected?" and "what is the significance?" for example, the bottom of page 11, top and middle of page 12 left me with these questions.

The number of figures has been reduced in the revised manuscript.

3) In the discussion starting on page 12, the initial statement that the experiments demonstrate that colloids attach to glass beads is an underwhelming start to the discussion. This observation has been made many times previously in other systems, and so is not a strong choice for starting the discussion.

This line is no longer used as the initial statement in the discussion section.

4) The discussion of the simulations (bottom of page 13) was hard to follow. On line 38 it is stated: "By making these two assumptions" but I could not determine what two assumptions were being discussed. Likewise, it was not clear where the "3.41" value (line 45) came from. I think this is a matter of the authors not providing a clear rationale for the manipulations being made.

The modeling section has been significantly revised to better provide a clear rationale for the manipulations being made.

5) The microspheres have a zeta potential of -44 mV. This indicates that they are actually carboxylate modified (or other negative functionality)? They are referred to only as "polystyrene".

The manuscript has been revised to indicate that the microparticles are sulfate modified polystyrene microparticles.

6) The statement "indicating that this episode of stress simulation caused the release of microspheres that were loosely retained" (Page 8, line 36) does not shed new light. Of course the microspheres amenable to release were the ones that were released. The statement appears to miss the intended mark.

This statement has been removed from the revised manuscript.

7) The statement: "The minimum and maximum pressures are negative" (page 9, line 6) is not clear. The corresponding figure does not indicate negative values or out of phase relationships, so it is not clear what the authors intend by this statement.

Figure does not indicate negative values because the plotted values have been normalized using the minimum and maximum pressures. The minimum and maximum

pressures used in the normalization are in fact negative (the actual values are provided in the text of the manuscript). Given that the statement appears to create unnecessary confusion on the part of the reviewer, it has been removed from the manuscript and the actual values of the minimum and maximum pressures used in the normalization are now provided without additional comment on their magnitudes.

The manuscript presents an interesting experimental study that serves to understand colloid mobilization in porous media using low-frequency elastic waves. The results are more applicable to induced waves, rather than seismic events, since the time frame of the studies is much longer than most seismic events. Induces waves are still interesting, since they are used in petroleum recovery and may be consider for some remediation approaches. In general the manuscript is well written, but there are some areas in which the methods are not fully described (e.g. modeling related to Figure 15). There is no significant theoretical underpinning for the experimental work, so it is unclear what one would do with these results in terms of trying to apply them to other situations. At this stage, the authors have elucidated some possible mechanisms, but there is clearly a need for more work to test these hypotheses.

Our goal with this manuscript is to introduce possible mechanisms for the release of colloids during seismic stimulation as a guide for future research. By presenting kinetic data (first order continuous and discrete, en masse releases) and microscopic observations of the mechanical behavior of the glass beads, we limit the mechanisms that need to be further investigated in future work.

The nature of the oscillations in pressure and temperature were not discussed at all. Given the 24-hr periodicity, they seem to be related more to some environmental control in the building than something related to the experiment. In any case, what is the relevance? If not relevant, why present this data? If relevant, why not discuss it? Why are they uncorrelated to the stimulations?

The relevance of the 24-hour periodicity is to demonstrate that most of the pressure fluctuations are due to environmental factors, not the stimulation of the column. Given the 24-hour period of the cycles, we anticipated it would be self-evident that the temperature and pressure readings were, for the most part, following an environmental diurnal cycle. As both reviewers misunderstood our interpretation of the 24-hour cycle and incorrectly assumed that we were implying a connection between the 24-hour cycle and the stimulation, we have revised the manuscript to clarify that no connection should be inferred.

The loading of colloids was quite high. Although these are small particles relative to the size of the beads, more than 16 pore volumes at a fairly high concentration were introduced. Why? Was this necessary for the visualization? Explain your reasoning, and whether this has an impact on the results. For example, if only 1 PV of colloids was loaded, would one see some of the oscillatory results?

The manuscript has been revised to state that the column was loaded with the colloidal dispersion until breakthrough was observed. It just so happened that 16 pore volumes of the colloidal dispersion were required for breakthrough. While

the proposed colloidal microparticle release mechanisms would still be present during stimulation of the column, it is unlikely that they would have been detected with only 1 PV of loading due to significant downstream portions of the column being unsaturated.

As was observed in the overall flowcell image (removed from the revised manuscript), the heaviest microparticle loading occurs near the inlet of the glass bead packing. Had only 1 PV of the colloidal dispersion been loading, it is unlikely that the entire column would have been loaded due to the absence of breakthrough. As such, there would have been a significant risk that microparticles released near the inlet during stimulation would be recaptured downstream in the unsaturated zone of the column.

Apparently the experiments were conducted only once. What are the error bars on the measurements? How reproducible are they?

The experiments were conducted only once. Please understand that it took months to setup the column and perform these experiments. Also, the data presented in the manuscript are only a small subset of the data collected and experiments performed. The reproducibility of the experiments is evident in the consistency of the data set. Error bars have been added to the third data set whose samples were analyzed in duplicate.

What was the rationale for selecting the frequency, stress level and length of the experiments?

The frequency was selected due to its ability to penetrate deep into the subsurface and thus its applicability to artificial seismic stimulation. The two stress amplitudes were selected to provide examples of first-order release kinetics only and first-order plus discrete, en masse release kinetics. The lengths of the experiments were selected to provide insight into the release kinetics.

Some specific comments:

1) P4 L43-5: the Results, the Conclusions.

O.K.

2) Report darcies in metric units

O.K.

3) Colloid concentrations should be reported in particles cm-3, or number cm-3.

O.K.

4) Were the zeta potentials presented in Fig. 1 measured by the authors? Methods? If these are negative, then should be -44 mV, not just 44 mV.

The manuscript has been revised to include the method used to measure the zeta potential. The "44 mV" has been corrected to "-44 mV."

5) Did the loading of colloids have any effect on permeability? Any change in pressure drop across the column?

The loading of colloids had no measurable effect on the permeability of the column (i.e. no measured change in the pressure drop).

6) The first experiment was quite long. This is not a seismic event. Why was it so long?

Whether or not the first experiment is a "seismic event" depends on the definition used. While the first experiment was longer than might be expected for a natural seismic event, it is not unreasonable to anticipate an artificial seismic event of such length as a method of enhanced oil recovery. The manuscript has been revised to indicate that we define both natural and artificial seismic events to be "seismic events" per the Merriam-Webster definition for "seismic."

The length of the first experiment was necessary to determine the shape of the decay curve (exponential) and thus the kinetics of the release mechanism (consistent with first order). This knowledge is vital when deciding if a proposed release mechanism should be considered further.

7) Why does the concentration in the release jump an order of magnitude as you go from 200 kPa to 350 kPa? Is there a threshold? At what point to do you go from low, simple exponential release to oscillatory behavior? Is this the energy needed to rotate the beads?

The Young's Modulus data indicate that an additional mechanism of compaction is triggered at higher stress amplitudes above a particular threshold. The threshold at which this additional mechanism of compaction is triggered will vary from system to system, depending to the degree of compaction before stimulation, the physical properties of the packing material (shape, coefficient of friction, etc.), and perhaps even the initial arrangement of the packing material. We believe that this additional mechanism is the occurrence of rotational cells within the column and is the cause of the oscillatory behavior observed in the microparticle effluent data - but further research is needed to confirm these beliefs.

8) Fig 9: note and discuss the regions with very low deposition of colloids near the outlet. This has clearly to do with the shape of the collector at the outlet, so even though you have the same cross-section, the flow is directed towards the center.

Figure 9 has been removed from the revised manuscript.

9) P11 L36: F missing in Figure.

Corrected.

10)Fig. 11: do the bare patches correspond to the contact with the top (and bottom) glass plates?

We suspect that the bare patches correspond to contact the top and bottom of the glass plates, but at this point we cannot say for certain. Many questions requiring further research, include ones surrounding the distribution of adsorbed microparticles, were raised by the flowcell experiments.

11)One can understand that these spherical beads will rotate if the frequency and stress applied are high enough (in fact there should be a particular frequency that would amplify this effect). However, in natural media there are many sharp edges, and presumably this effect would be much smaller. This should be mentioned in the discussion and conclusions. The results may be an artifact of the simplicity of this system.

Natural materials would be expected to undergo fewer rotations than the idealized system reported in this manuscript. However, the concentration of stresses caused by their sharp edges and irregular shapes is anticipated to result in similar colloidal microparticle releases. In addition, consolidated materials such as sandstone that might not exhibit the same amount of rotations as loose granular materials are known to experience microfracturing and grain crushing during compaction. We have revised the manuscript to highlight these facts and to explain that we are using a simple system because the concentration oscillations were previously observed in natural systems of sand and sandstone and we wished to eliminate the variability in the natural systems as a source of the oscillatory behavior.

12)P13 L31: The oscillations also occurred in the low stress stimulations, but were much smaller. Instead of "only occurred" it would be better to say "were magnified."

Corrected.

13)P13 L36: I would cross-out "fully."

Corrected.

14)P13 L41 to P14 L15: This should be described in the Methods section, the results presented in the Results section, and only discussed here, in keeping with the organization of the paper. The simple first-order decay model is clear, but it is unclear how they model the discrete events. Describe more fully in the Methods section. Is Fig.15 comparing experimental to model? Unclear.

The manuscript has been substantially revised and reorganized. We consider the new presentation to be consistent with the new organization. The model is more clearly described.

15)P15 L57: hurdle

Corrected.

16)P17 L5-7: Clogging does not really explain the oscillatory release, as discussed, so it should not be presented here as an equal mechanism to grain rearrangement. Also, add caution to results given the simple geometry of the spheres.

Clogging is no longer presented as an equal mechanism to grain rearrangement. The manuscript has been revised to more strongly emphasize that we have observed the oscillatory releases in systems of natural sand and sandstone.